

## Supporting Information

### Hydrothermal Microwave Synthesis of $\text{Co}_3\text{O}_4/\text{In}_2\text{O}_3$ Nanostructures for Photoelectrocatalytic Reduction of Cr(VI)

JieJie Nan,<sup>a</sup> Sijia Guo<sup>a</sup>, Dalal Alhashmialameer,<sup>b</sup> Qingming He,<sup>a</sup> Yinuo Meng,<sup>a</sup> Ruixiang Ge,<sup>a,\*</sup> Salah M. El-Bahy,<sup>c</sup> Nithesh Naik,<sup>d</sup> Vignesh Murugadoss,<sup>e</sup> Mina Huang,<sup>c,f</sup> Ben Bin Xu,<sup>g</sup> Qian Shao,<sup>a,\*</sup> Zhanhu Guo<sup>e,\*</sup>

<sup>a</sup> College of Chemical and Biological Engineering, Shandong University of Science and Technology, Qingdao 266590, China

<sup>b</sup> Department of Chemistry, College of Science, Taif University, P.O.Box 11099, Taif 21944, Saudi Arabia

<sup>c</sup>Department of Chemistry, Turabah University College, Taif University, P.O.Box 11099, Taif 21944, Saudi Arabia

<sup>d</sup>Department of Mechanical & Manufacturing Engineering, Manipal Institute of Technology, Manipal Academy of Higher Education, Manipal-576104, Karnataka, India

<sup>e</sup> Integrated Composites Laboratory (ICL), Department of Chemical and Biomolecular Engineering, University of Tennessee, Knoxville, TN, 37996, USA

<sup>f</sup> College of Materials Science and Engineering, Taiyuan University of Science and Technology, Taiyuan, 030024, China

<sup>g</sup> Department of Mechanical and Construction Engineering, Faculty of Engineering and Environment, Northumbria University, Newcastle upon Tyne, NE1 8ST, UK

\*Corresponding authors: [ruixiang\\_ge@sina.com](mailto:ruixiang_ge@sina.com) (R. Ge); [shaoqian@sdust.edu.cn.com](mailto:shaoqian@sdust.edu.cn.com) (Q. Shao); [zguo10@utk.edu](mailto:zguo10@utk.edu) or [nanomaterials2000@gmail.com](mailto:nanomaterials2000@gmail.com) (Z. Guo)

## Materials

$\text{Co}(\text{NO}_3)_2 \cdot 6\text{H}_2\text{O}$  was obtained from Chengdu Kelong Chemical Co., Ltd.  $\text{In}(\text{NO}_3)_3 \cdot 4.5\text{H}_2\text{O}$  was provided by Sinopharm Chemical Reagent Co., Ltd. (AR, Shanghai, China).  $\text{CO}(\text{NH}_2)_2$  was bought from Tianjin Damao Chemical Reagent Factory (AR, Tianjin, China). P-benzoquinone, isopropyl alcohol (IPA), EDTA-2Na, and silver nitrate ( $\text{AgNO}_3$ ) were provided by Chengdu Kelong Co. Ltd. (AR, Chengdu, China). All the chemicals were used without any further purification. The nickel foam used in the experiment was purchased from Suzhou Sheng Er no Technology Co., Ltd. Cr(VI) solutions for PEC degradation experiments were prepared in deionized water.

## Material Characterization

The crystalline phases ( $20^\circ$ - $80^\circ$ ) of the samples were determined by X-ray diffraction (XRD, ultima IV, Rigaku, Japan) with Cu  $K\alpha$  radiation ( $\lambda = 0.1540$  nm) at a scanning rate of 8/min. The information of microstructure and elemental mapping of the products were tested by scanning electron microscope (SEM, S-4800, Hitachi, Japan). Transmission electron microscopy was measured using a JEOL JEM-2100F system (TEM, JEM-2100F, Japan) at an accelerating voltage of 200 kV. The Brunauer–Emmett–Teller (BET) results were obtained at 77.350 K using a micropolitics surface area and pore volume analyzer (TriStar II 3020, USA). The UV–Vis diffuse reflectance spectra of the samples were analyzed by UH4150 UV–Vis spectrophotometer (Hitachi, Japan). The photoluminescence spectra (PL) were obtained by Hitachi F-4600 (Hitachi, Japan). Elemental composition information of samples was examined by an ESCALAB 250Xi X-ray photoelectron spectrometer (XPS, Thermo Scientific, USA). The transient photocurrent and electrochemical impedance spectroscopy (EIS) were analyzed using an electrochemical workstation (Autolab, Metrohm Co. Ltd.). Cyclic voltammetric electrochemical measurements were carried out on a CHI760E electrochemical

workstation (Shanghai Chenhua Instruments Co., Ltd., China). The  $\zeta$ -potential was analyzed by a microiontophoresis apparatus (Powereach, JS94H, China).

### **PEC performance tests**

The PEC activity was evaluated by reduction of Cr(VI). The synthesized  $\text{Co}_3\text{O}_4/\text{In}_2\text{O}_3$  composites were loaded on nickel foam as photoelectrodes. The PEC experiments were carried out by a three-electrode setup, with the obtained PEC electrode ( $2 \times 2.5 \text{ cm}^2$ ), platinum (Pt) sheet, and the saturated calomel electrode (SCE) serves as the working electrode, the counter electrode, and the reference electrode, respectively. Before the PEC tests, the electrodes were immersed into the Cr(VI) solution (10 mg/L  $\text{K}_2\text{Cr}_2\text{O}_7$ , 100 mL) for 30 min under a dark condition to reach the adsorption-desorption equilibrium. The PEC reduction experiments were carried out under a certain bias voltage (0-1 V) and irradiation of a 200 W xenon lamp in the wavelength range of 320-1100 nm as the visible light source. During the PEC reaction, 2 mL of the reaction solution was aspirated with a pipette every 20 min, which was further analyzed by a ultraviolet-visible spectrograph (UV9000) at 540 nm based on 1,5-diphenylcarbodihydrazide spectrophotometry to determine the concentration of Cr(VI) in the solution.<sup>1</sup> To eliminate the interference of adsorption, the concentration of Cr(VI) after 30 min of adsorption in dark was used as the initial concentration for PEC reaction. All PEC reduction tests were performed at pH=2.

### **Effect of pH on the reduction of Cr(VI):**

To investigate the effect of pH Cr(VI) reduction, we measured the zeta potential of the composite  $\text{Co}_3\text{O}_4/\text{In}_2\text{O}_3$  at different pH. As shown in Figure S1, the zeta potential at pH=2 is higher than that at pH=4, pH=6, and pH=8. The  $\text{HCrO}_4^-$  in the solution dominates with the increase of pH, which causes the positive charge on the surface of the sample to be gradually decreased. Therefore, when the solution pH is further increased, the

electrostatic adsorption between the catalyst  $\text{Co}_3\text{O}_4/\text{In}_2\text{O}_3$  surface and  $\text{Cr(VI)}$  ions decreases, thus decreasing the reduction of  $\text{Cr(VI)}$  ion reduction ability. Previous reports claim that the reduced ability of  $\text{Cr(VI)}$  ions is stronger at acidic  $\text{pH} = 2-3$ .<sup>2, 3</sup> Thus, in the present work, the solution  $\text{pH}$  was set as 2.

The solution  $\text{pH}$  may affect the catalytic activity for  $\text{Cr(VI)}$  reduction in two ways. First, the solution  $\text{pH}$  will affect the distribution of charge on the catalyst surface, where the catalyst  $\text{Co}_3\text{O}_4/\text{In}_2\text{O}_3$  has a positive charge on the surface, enabling a larger number of negatively charged chromium anions to be adsorbed on the catalyst surface and hence reduced. Second, the second aspect of the effect of  $\text{pH}$  on the rate of  $\text{Cr(VI)}$  reduction is that  $\text{pH}$  affects the form of  $\text{Cr(VI)}$  present in the solution.  $\text{Cr(VI)}$  is present in solution as acid ions, mainly as  $\text{HCrO}_4^-$  and  $\text{H}_2\text{CrO}_4$  in acidic solutions, with a very small distribution of  $\text{Cr}_2\text{O}_7^{2-}$ . All three ions or molecules have a strong electron gaining ability. When the  $\text{pH}$  is higher than 6,  $\text{Cr(VI)}$  mainly exists in the form of  $\text{CrO}_4^{2-}$ , and the electron gaining the ability of  $\text{Cr(VI)}$  declines sharply at this time, so the reduction rate of  $\text{Cr(VI)}$  is decreased significantly when the initial  $\text{pH}$  is higher than 6.

### **Bandgap energy:**

As indirect bandgap semiconductors, the optical band gaps of  $\text{Co}_3\text{O}_4$  and  $\text{In}_2\text{O}_3$  are calculated by the Kubelka-Munk equation:<sup>4</sup>

$$(\alpha h\nu)^2 = k(h\nu - E_g)$$

where  $\alpha$ ,  $k$ ,  $h\nu$  and  $E_g$  denote the absorption coefficient, the proportionality constant, the photon energy, and the bandgap energy, respectively. For the semiconductor pure  $\text{Co}_3\text{O}_4$  particles and  $\text{In}_2\text{O}_3$  particles, the forbidden bandwidths are 1.40 and 2.81 eV, respectively, consistent with the previously reported values for  $\text{Co}_3\text{O}_4$  and  $\text{In}_2\text{O}_3$ ,<sup>5, 6</sup> which are depicted in Figure S7.

**Table S1.** Abbreviation for other mole ratio information and materials In/Co.

In (NO <sub>3</sub> ) <sub>3</sub> · 4.5 H <sub>2</sub> O(g)	Co(NO <sub>3</sub> ) <sub>2</sub> · 6H <sub>2</sub> O(g)	n(In):n(Co)	Abbreviation
0	1.455	/	Co <sub>3</sub> O <sub>4</sub> particle
1.910	0	/	In <sub>2</sub> O <sub>3</sub> particle
0.057	1.455	0.03:1	CI-3%-450
0.095	1.455	0.05:1	CI-5%-450
0.134	1.455	0.07:1	CI-7%-450

**Table S2.** Specific surface area, pore size and pore volume of samples.

Samples	Surface area S <sub>BET</sub> (m <sup>2</sup> g <sup>-1</sup> )	Pore size (nm)	Pore volume (cm <sup>3</sup> g <sup>-1</sup> )
Co <sub>3</sub> O <sub>4</sub>	9.51	4.77	0.01
In <sub>2</sub> O <sub>3</sub>	25.76	9.52	0.06
CI-5%-350	47.00	10.07	0.12
CI-5%-400	32.72	10.74	0.09
CI-5%-450	25.65	10.31	0.07
CI-5%-500	19.79	7.58	0.04
CI-5%-550	18.75	7.27	0.03

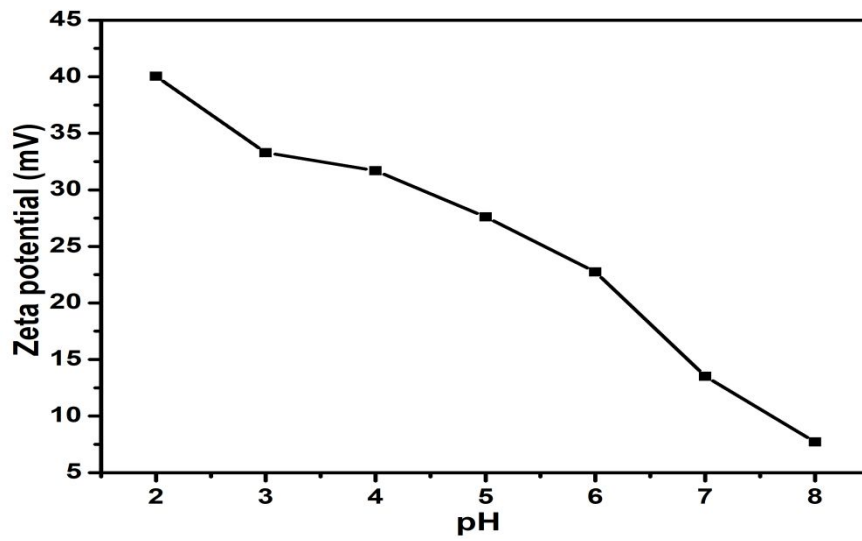


**Figure S1.** Zeta potential of CI-5%-400 under different pH.

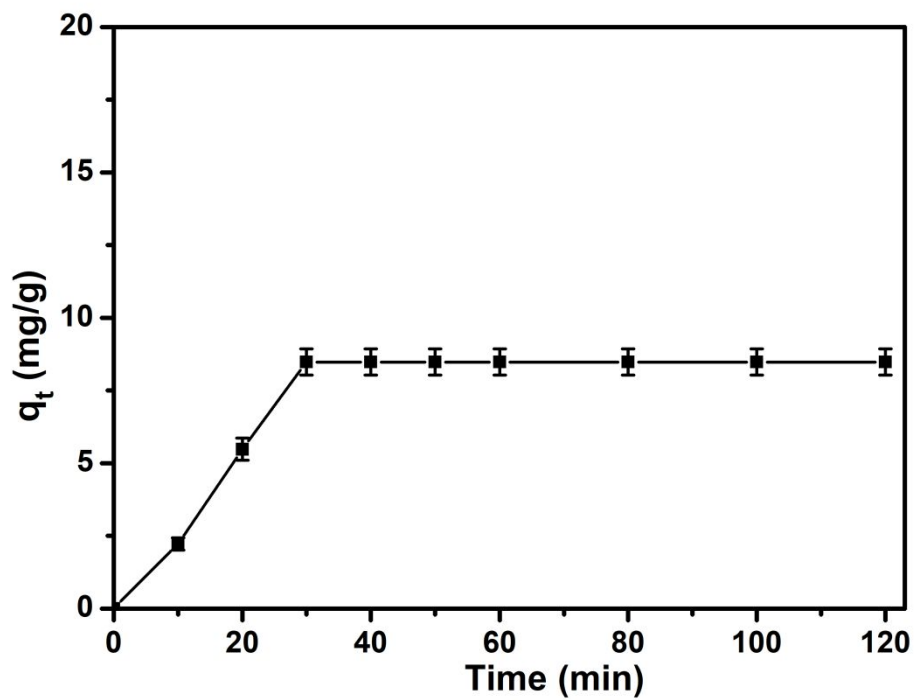


**Figure S2.** The effect of adsorption on Cr(VI) reduction. (Experimental conditions: amount of adsorbent = 30 mg, Cr(VI) ion concentration = 10 mg/L, volume of solution = 100 mL, adsorption temperature = 25° C, pH = 2).

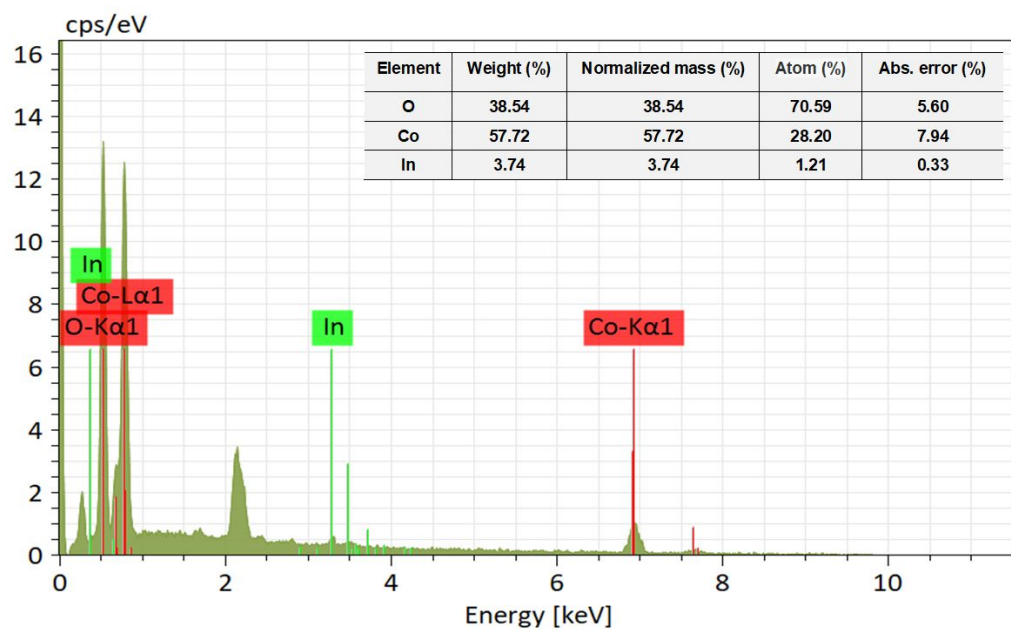


Figure S3. EDS measurement of the plotted area of CI-5%-400.

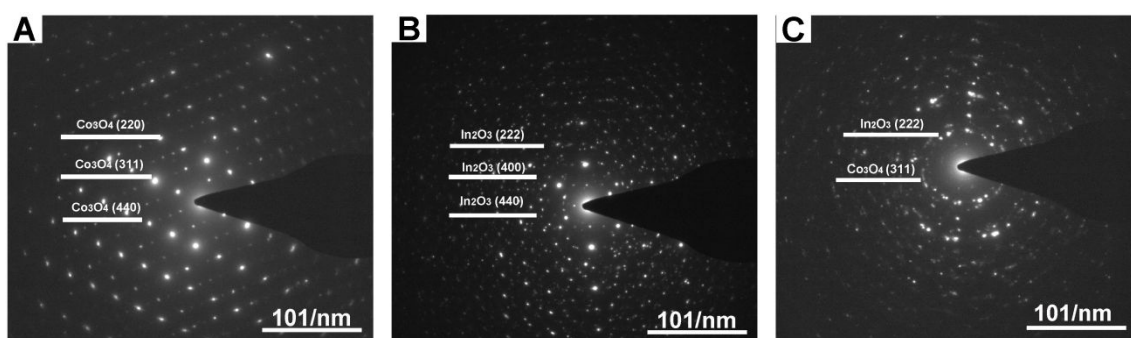


Figure S4. SAED patterns of (A)  $\text{Co}_3\text{O}_4$ , (B)  $\text{In}_2\text{O}_3$ , (C) CI-5%-400.

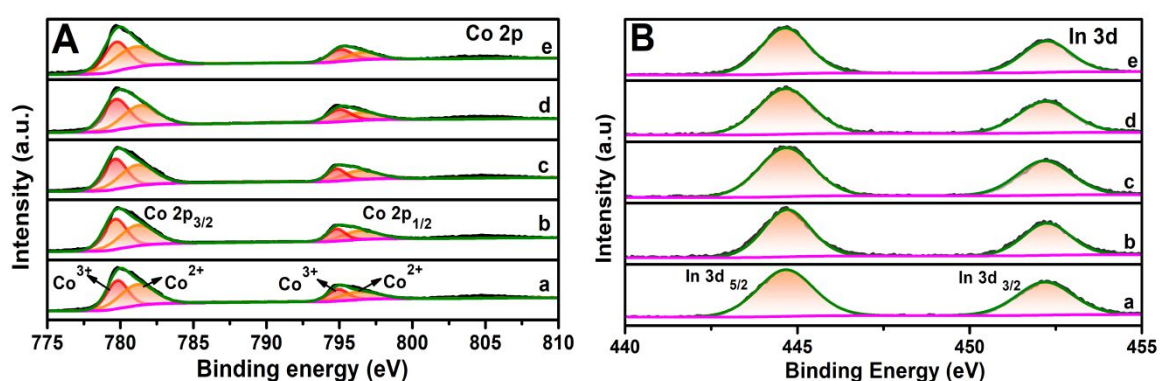
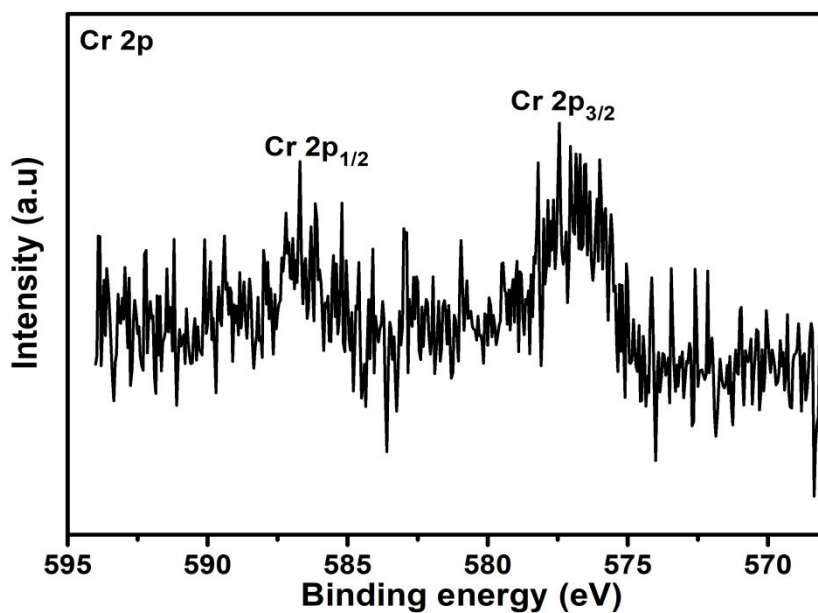
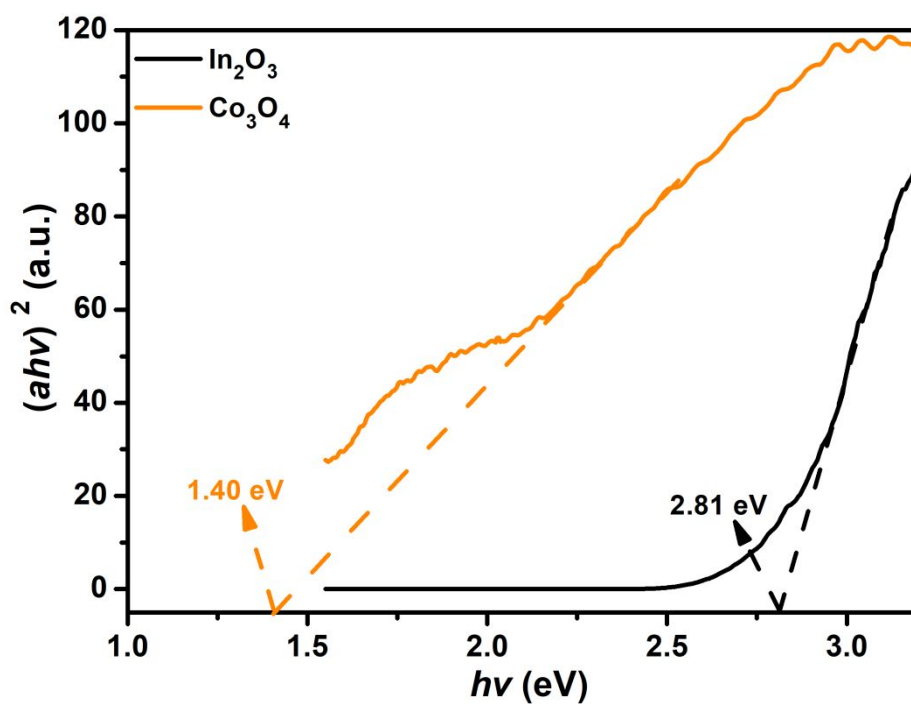


Figure S5. XPS spectra of (A) Co 2p and (B) In 3d for the  $\text{Co}_3\text{O}_4/\text{In}_2\text{O}_3$  composites: (a) CI-5%-350, (b) CI-5%-400, (c) CI-5%-450, (d) CI-5%-500 and (e) CI-5%-550.



**Figure S6.** Cr 2p high-resolution XPS spectra of  $\text{Co}_3\text{O}_4/\text{In}_2\text{O}_3$  composites after photoelectrocatalytic reduction of Cr(VI).



**Figure S7.** The Tauc plots of  $\text{Co}_3\text{O}_4$  and  $\text{In}_2\text{O}_3$ .

## References

- (1) Zhang, Y.; Jing, C.; Zheng, J.; Yu, H.; Chen, Q.; Guo, L.; Pan, D.; Naik, N.; Shao, Q.; Guo, Z. Microwave Hydrothermal Fabrication of Cufecr Ternary Layered Double Hydroxides with Excellent Cr(VI) Adsorption. *Colloids Surf., A* **2021**, *628*, 127279.
- (2) Li, Y.; Gao, Y.; Zhang, Q.; Wang, R.; Li, C.; Mao, J.; Guo, L.; Wang, F.; Zhang, Z.; Wang, L. Flexible and Free-Standing Pristine Polypyrrole Membranes with a Nanotube Structure for Repeatable Cr(VI) Ion Removal. *Sep. Purif. Technol.* **2021**, *258*, 117981.
- (3) Zhao, H.; Xia, Q.; Xing, H.; Chen, D.; Wang, H. Construction of Pillared-Layer Mof as Efficient Visible-Light Photocatalysts for Aqueous Cr(VI) Reduction and Dye Degradation. *ACS Sustainable Chem. Eng.* **2017**, *5*, 4449-4456.
- (4) Sun, L.; Shao, Q.; Zhang, Y.; Jiang, H.; Ge, S.; Lou, S.; Lin, J.; Zhang, J.; Wu, S.; Dong, M.; Guo, Z. N Self-Doped ZnO Derived from Microwave Hydrothermal Synthesized Zeolitic Imidazolate Framework-8 toward Enhanced Photocatalytic Degradation of Methylene Blue. *J. Colloid Interface Sci.* **2020**, *565*, 142-155.
- (5) Peng, L.; Xiao, Y.; Wang, X. I.; Feng, D. w.; Yu, H.; Dong, X. t. Realization of Visible Light Photocatalysis by Wide Band Gap Pure SnO<sub>2</sub> and Study of In<sub>2</sub>SnO<sub>2</sub> Photolysis Catalyst. *ChemistrySelect* **2019**, *4*, 8460-8469.
- (6) Turan, E.; Zeybekoğlu, E.; Kul, M. Effects of Bath Temperature and Deposition Time on Co<sub>3</sub>O<sub>4</sub> Thin Films Produced by Chemical Bath Deposition. *Thin Solid Films* **2019**, *692*, 137632.